

# Nanocrystalline NiO hollow spheres in conjunction with CMC for lithium-ion batteries

Chao Zhong · Jia-Zhao Wang · Shu-Lei Chou · Konstantin Konstantinov · Mokhlesur Rahman · Hua-Kun Liu

Received: 16 June 2009 / Accepted: 27 March 2010 / Published online: 11 April 2010  
© Springer Science+Business Media B.V. 2010

**Abstract** Hollow spherical NiO particles were prepared using the spray pyrolysis method with different concentrations of precursor. The electrochemical properties of the NiO electrodes, which contained a new type of binder, carboxymethyl cellulose (CMC), were examined for comparison with NiO electrodes with polyvinylidene fluoride (PVDF) binder. The electrochemical performance of NiO electrodes using CMC binder was significantly improved. For the cell made from 0.3 mol L<sup>-1</sup> precursor, the irreversible capacity loss between the first discharge and charge is about 43 and 24% for the electrode with PVDF and CMC binder, respectively. The cell with NiO–CMC electrode has a much higher discharge capacity of 547 mAh g<sup>-1</sup> compared to that of the cell with NiO–PVDF electrode, which is 157 mAh g<sup>-1</sup> beyond 40 cycles.

**Keywords** Spray pyrolysis · Nickel oxide anode · CMC binder · Lithium-ion batteries

## 1 Introduction

Although carbon-based materials are the accepted anode used in the majority of commercial lithium-ion batteries, various new higher capacity anode materials are still being studied to meet the increasing energy demands of modern devices, especially electric and hybrid electric vehicles. Among the most attractive candidates, transition-metal oxides could be a new class of promising anode materials

for lithium-ion batteries. The transition metal oxides react reversibly with lithium in lithium cells below 1.5 V and demonstrate large capacity (about 700 mAh g<sup>-1</sup>) and long cycle life [1]. Nickel oxide, NiO, has recently been intensively studied as an anode material.

NiO can be prepared through various methods, such as microwave-assisted and liquid oxidation combination techniques [2], the plasma assisted oxidation method [3], and the molten-salt assisted oxidation route [4]. These preparation methods are, however, very complicated and difficult to control. The spray pyrolysis technique, by comparison, has several advantages. It represents a simple and low-cost alternative for producing large-scale sub-micron-/nano-particles with controlled composition and morphology, good crystallinity, and uniform size distribution, all of which can be readily obtained in only one step.

In order to enhance the performance of lithium-ion batteries, researchers and battery manufacturers are not only trying to create new electrode materials, but also searching for new binders, since battery efficiency is strongly dependent on the electrode engineering [5, 6]. Recent studies have shown that some binders used for electrode preparation influence the electrochemical performance of the batteries [7, 8]. The most common binder used in Li-ion batteries is poly(vinylidene)fluoride, PVDF. The mechanical and electrochemical properties of PVDF are a good compromise between the multiple criteria described above. However, using PVDF has the following drawbacks:

- PVDF is only soluble in organic solvents, and it is expensive and dangerous to humans and the environment;
- Control of the humidity (less than 2%) is needed during the electrode preparation.

Recently, aqueous binders have gradually replaced PVDF binder for the anode material [9–12]. The advantages of

C. Zhong · J.-Z. Wang (✉) · S.-L. Chou · K. Konstantinov · M. Rahman · H.-K. Liu  
Institute for Superconducting and Electronic Materials, ARC  
Center of Excellence for Electromaterials Science, University of  
Wollongong, Wollongong, NSW 2519, Australia  
e-mail: jiazhaow@uow.edu.au

aqueous binders are [13]: (1) low cost, (2) no pollution problems, and (3) no requirement for strict control of the processing humidity. Among the various water soluble binders, carboxymethyl cellulose (CMC) is the most attractive binder for improving battery performance. CMC is soluble in environmentally friendly solvents such as water [14], which is of importance for future electrode production.

In this research work, we prepared NiO by a simple spray pyrolysis method. NiO electrode using CMC binder is being reported for the first time. The capacity and cycling stability are improved significantly compared with the results published previously, in which the NiO electrodes contained PVDF as the binder [15].

## 2 Experimental

Nanocrystalline NiO powders were synthesized by a spray pyrolysis method [16]. Nickel oxide powder was prepared using 0.1, 0.3, and 0.5 mol L<sup>-1</sup> aqueous solutions of nickel nitrate hexahydrate,  $\text{Ni}(\text{NO}_3)_2 \cdot 6\text{H}_2\text{O}$  (Aldrich Chemicals). The solution was peristaltically pumped into a three-zone spray pyrolysis furnace with the operating temperature at 700 °C, using compressed air as the carrier gas. The resultant powder was separated from the hot gas stream via a collecting jar and collected into airtight sample bottles.

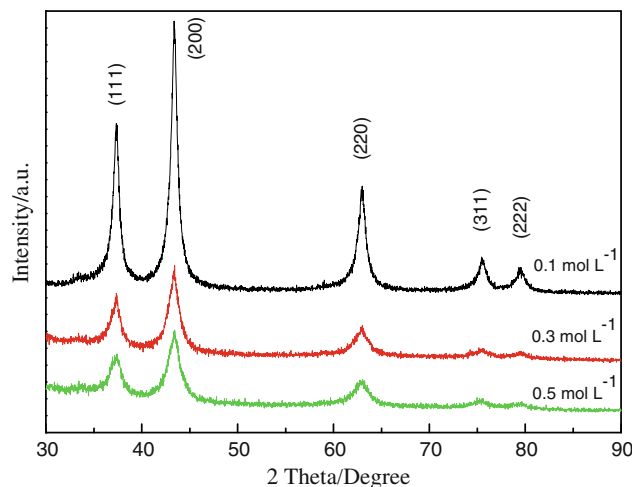
Phase analysis was performed by powder X-ray diffraction (XRD) using a Phillips 1730 X-ray generator and diffractometer with Cu K $\alpha$  radiation. The morphologies of the NiO powders were investigated by scanning electron microscopy (SEM; JEOL JEM-3000, 30 kV), field emission SEM (FE-SEM; JEOL JSM-7500F), and transmission electron microscopy (TEM; JEOL 2011, 200 kV). The electrodes with different binders were studied by SEM before and after cycling.

To fabricate the NiO electrodes, 70 wt% NiO powder was mixed with 20 wt% carbon black and 10 wt% binder, which was either sodium carboxymethyl cellulose (CMC, average Mw: 250,000, Aldrich) or poly (vinylidene)fluoride (PVDF, average Mw: 534,000, Aldrich), using deionized water or *N*-methyl-2-pyrrolidinone (NMP) as the respective solvents. The electrochemical characterizations were carried out using CR 2032 coin-type cells, which were assembled in an Ar-filled glove box (Mbraun, Unilab, Germany) by stacking the NiO anodes with a porous polypropylene separator and a lithium foil counter and reference electrode. The electrolyte used was 1 M LiPF<sub>6</sub> in a 50:50 (v/v) mixture of ethylene carbonate (EC) and dimethyl carbonate (DMC). The cells were galvanostatically discharged and charged at a current density of 100 mA g<sup>-1</sup>. The discharge capacities are based on the amount of active material in the electrodes.

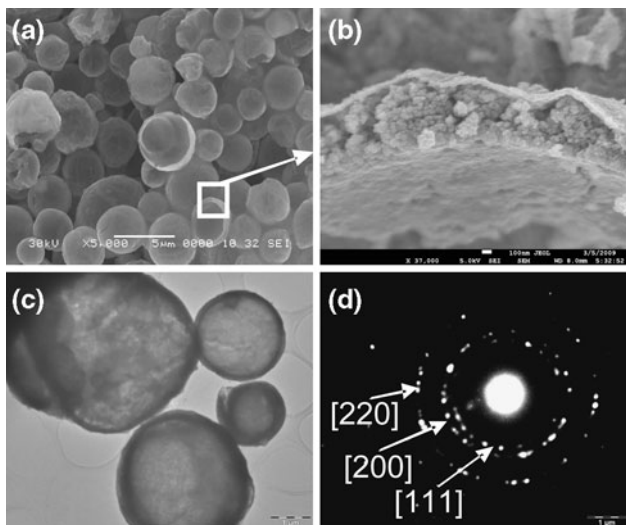
## 3 Results and discussion

Figure 1 shows the XRD patterns of the NiO powders prepared by the spray pyrolysis method at 700 °C using the solutions of  $\text{Ni}(\text{NO}_3)_2 \cdot 6\text{H}_2\text{O}$  with concentrations of 0.1, 0.3, and 0.5 mol L<sup>-1</sup>, respectively. All the diffraction peaks correspond well with standard crystallographic data (Joint Committee on Powder Diffraction Standards (JCPDS) File No. 04-0835). The structure is that of a cubic unit cell with diffraction peaks at 37.38°, 43.38°, 62.92°, 75.28°, and 79.48°. The XRD peaks for the NiO powders are very broad, indicating their nanocrystalline nature. The average crystal sizes of the NiO powders were determined by using the Traces software package and the Scherrer formula. The crystal sizes are 10.52, 3.99, and 3.27 nm for the NiO samples sprayed from solutions of 0.1, 0.3, and 0.5 mol L<sup>-1</sup>, respectively. The crystal size of the NiO powders was reduced when the concentration was increased. The results indicate that pure nanocrystalline NiO powders with very small crystal sizes can be prepared by the simple spray pyrolysis method.

An SEM image of the NiO powders prepared from the 0.3 M solution is shown in Fig. 2a. The particles are mainly spherical agglomerates, which is a typical structure for this spray process, with sizes in the range of 2–4 μm. From the broken spherical particles, it can be seen that the particles are spherical hollow balls. It also can be seen from FE-SEM (Fig. 2b) that the wall thickness ranges from 300 to 500 nm. The spherical hollow balls are composed of small spheroidal particles with sizes of 20–50 nm. The hollow spherical structure is further confirmed by TEM (Fig. 2c). In the selected-area electron diffraction (SAED) pattern presented in Fig. 2d, all of the electron diffraction rings can be indexed to cubic phase NiO, which also agrees



**Fig. 1** X-ray diffraction patterns for NiO powders from spray pyrolysis solutions at different concentrations



**Fig. 2** Images of NiO powder made from 0.3 M precursor: **a** SEM, **b** FE-SEM, **c** TEM, and **d** corresponding SAED pattern to **c**

very well with the XRD analysis. The Brunauer–Emmett–Teller (BET) results made it clear that an increase in the concentration of the precursor solution caused a pronounced decrease in the BET specific surface area,  $S_{\text{BET}}$ . The powder obtained from the 0.1 mol L<sup>-1</sup> solution exhibits a remarkably high  $S_{\text{BET}}$  value of 42.4 m<sup>2</sup> g<sup>-1</sup>. The powders prepared using 0.3 and 0.5 mol L<sup>-1</sup> solutions have values of only 10.5 and 9.7 m<sup>2</sup> g<sup>-1</sup>, respectively.

Figure 3 shows discharge capacities versus cycle number for cells made using NiO electrodes, where the NiO was sprayed from different concentrations of the precursor solution, and the two different binders. When using PVDF as a binder, it was found that the capacities for all the samples were high for the first few cycles; however, the

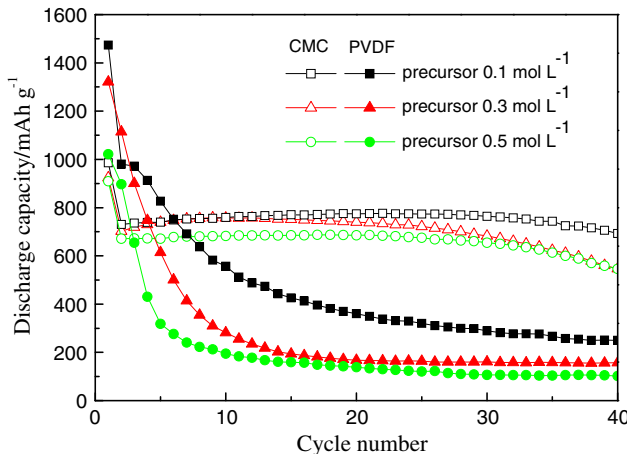


**Fig. 3** Discharge capacities versus cycle number for NiO electrodes made from spray solutions at different concentrations with PVDF and CMC binders

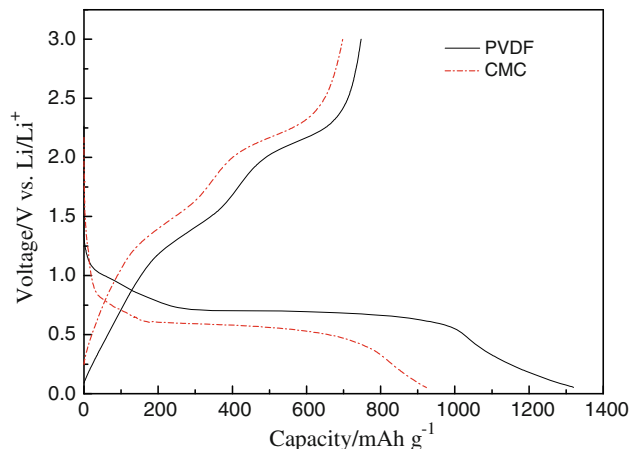


**Fig. 4** Typical charge–discharge curves for NiO electrodes (0.3 mol L<sup>-1</sup>) with CMC and PVDF binders

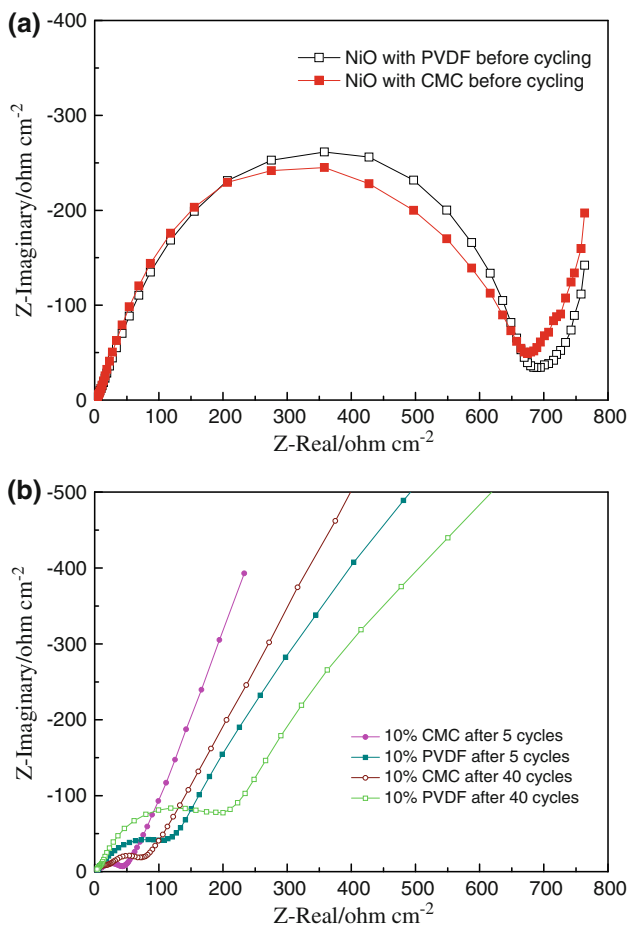
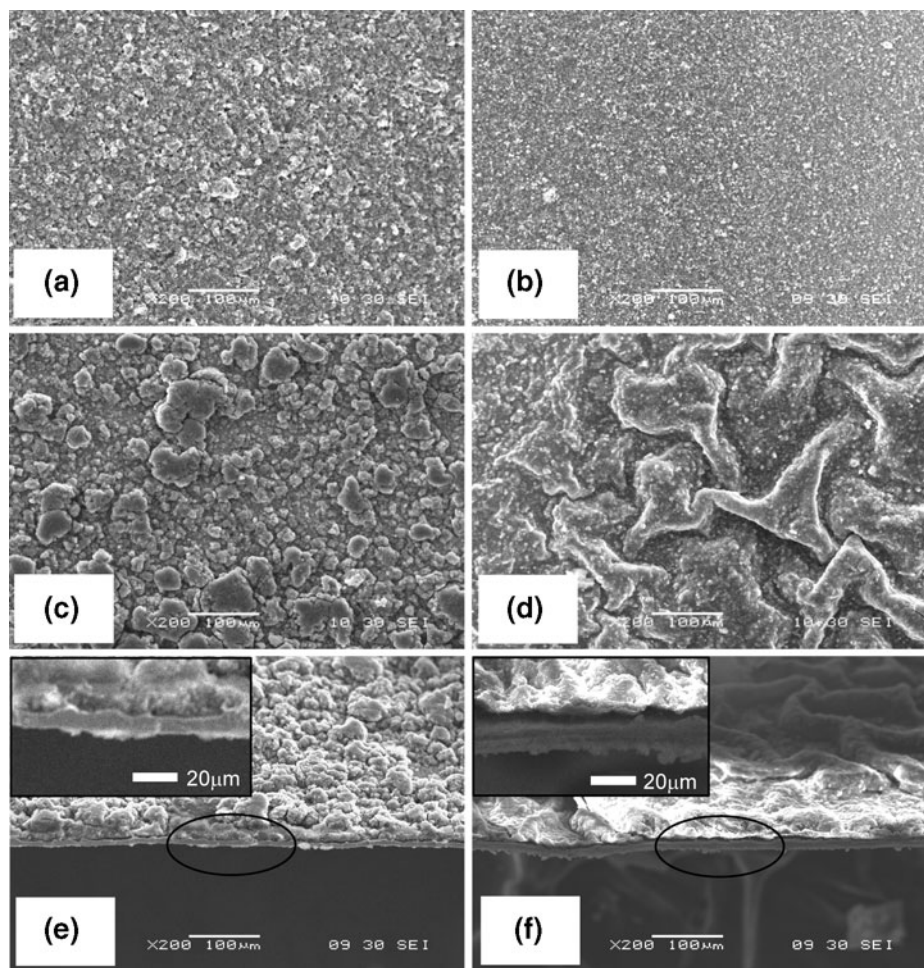


**Fig. 5** Nyquist impedance plots of NiO electrodes (0.3 mol L<sup>-1</sup>) with different binders **(a)** before and **(b)** after cycling

discharge capacities decreased dramatically over 10 cycles and only showed 250, 157, and 102 mAh g<sup>-1</sup> (for the 0.1, 0.3 and 0.5 mol L<sup>-1</sup> precursor concentrations, respectively) after 40 cycles. This phenomenon has been reported

**Fig. 6** SEM images of NiO electrodes ( $0.3 \text{ mol L}^{-1}$ ) with CMC binder (left) and PVDF binder (right): **a, b** before cycling; **c, d** after cycling; **e, f** cross-sections of electrodes after cycling. Insets in **e** and **f** show enlargements of the indicated areas



in previous publications [15]. In order to improve the cycling stability of the NiO samples prepared by the spray pyrolysis method, CMC binder was tested using the as-prepared NiO powders. The cycling stabilities of the cells with CMC are obviously improved. The NiO electrodes made from 0.1, 0.3 and 0.5 mol L<sup>-1</sup> precursor concentrations using CMC as the binder demonstrate capacities as high as 693, 547 and 545 mAh g<sup>-1</sup>, respectively, after 40 cycles, which is an obvious improvement compared to the electrodes using PVDF binder. Typical charge-discharge curves of the cells made from the 0.3 mol L<sup>-1</sup> precursor concentration with the two different binders are presented in Fig. 4. The first discharge capacities of the NiO electrodes with PVDF and CMC binders are 1320 and 924 mAh g<sup>-1</sup>, and the first charge capacities of these NiO electrodes are 747 and 698 mAh g<sup>-1</sup>, respectively. The irreversible capacity loss between the first discharge and the first charge is about 43 and 24% for the electrodes with PVDF and CMC binders, respectively. These results confirm that the binder is an important issue affecting the cycling stability [8, 12].

To investigate the relationship between the ac impedance spectra and the cycling behaviors of electrodes with different binders, we carried out electrochemical impedance spectroscopy (EIS) tests on the NiO electrodes made from the 0.3 mol L<sup>-1</sup> precursor solution before cycling, after 5 charge-discharge cycles, and after 40 cycles. The Nyquist impedance plots of the NiO electrodes with different binders before and after cycling are presented in Fig. 5. Generally, the high frequency semicircle and the semicircle in the medium-frequency region are attributed to the solid electrolyte interphase (SEI) film and/or contact resistance, and the Li<sup>+</sup> charge-transfer impedance on the electrode/electrolyte interface, respectively. The inclined line at an approximate 45° angle to the real axis corresponds to the lithium-diffusion processes within the electrode [17]. From Fig. 5a, it can be clearly seen that the diameters of the semicircles in the medium-frequency region are similar before cycling for the two electrodes, regardless of the binder. However, the diameters of the semicircles for electrodes with CMC binder are smaller than for the electrodes with PVDF binder after 5 and 40

cycles (Fig. 5b). The results indicate that the charge-transfer resistance of the cell with NiO/CMC electrode is much lower than that of the cell made from NiO/PVDF. This phenomenon may be the reason why the capacity and cycling stability of the cell with CMC are much better compared to the cell with PVDF binder (see Fig. 3).

In order to explore the reasons why the charge-transfer resistance is higher in the cell with PVDF binder after cycling, a morphological study of the electrodes before cycling and after 40 cycles was conducted (Fig. 6). As can be seen, the electrode material is expanded and creased after cycling for the cell with PVDF binder, while the electrode particles of the cell with CMC are just slightly agglomerated compared to the electrode before cycling (Fig. 6a–d). The images of the electrode cross-sections show that the electrode material with CMC has remained adhered to the copper foil, while a big gap is found between the active material and the substrate for the electrode with PVDF after 40 cycles (Fig. 6e, f).

#### 4 Conclusions

Nanocrystalline NiO hollow spheres were synthesized by the spray pyrolysis method using different concentrations of precursor solution and tested as anode materials with CMC and PVDF binders. The as-prepared material obtained from a lower concentration of precursor has a larger BET specific surface area and therefore gives better electrochemical performance. It was also found that the capacity and cycling stability of the electrode using CMC binder are significantly improved compared to the electrode with PVDF binder. The preliminary results reported here provide useful information for further research on exploring new environmentally friendly water soluble binders to replace the conventional organic solvent based binders for battery applications.

**Acknowledgements** Financial support provided by the Australian Research Council (ARC) through ARC Center of Excellence funding and an ARC Discovery Project (DP 0987805) is gratefully acknowledged. Electrochemistry testing assistance provided by Fábio R. Bento and Hu Zhou is highly appreciated. Many thanks also go to Dr. T. Silver for critical reading of the manuscript.

#### References

1. Poizot P, Laruelle S, Gruegeon S, Dupont L, Tarascon JM (2000) *Nature* 407:496
2. Lai TL, Shub YY, Huang GL, Lee CC, Wang CB (2008) *J Alloys Compd* 450:318
3. Varghese B, Reddy MV, Yanwu Z, Lit CS, Hoong TC, Rao GVS, Chowdari BVR, Wee ATS, Lim CT, Sow CH (2008) *Chem Mater* 20:3360
4. Zheng YZ, Zhang ML (2007) *Mater Lett* 61:3967
5. Broussely M (1999) *J Power Sources* 81–82:140
6. Zhang X, Ross PN, Kostecki R, Kong F, Sloop S, Kerr JB, Striebel K, Cairns EJ, McLarnon F (2001) *J Electrochem Soc* 148:A463
7. Buqa H, Holzapfel M, Krumeich F, Veit C, Novak P (2006) *J Power Sources* 161:617
8. Drofenik J, Gaberscek M, Dominko R, Poulsen FW, Mogensen M, Pejovnik S, Jamnik J (2003) *Electrochim Acta* 48:883
9. Pejovnik S, Bele RD, Gaberscek M, Jamnik J (2008) *J Power Sources* 184:593
10. Li J, Dahn HM, Krause LJ, Le DB, Dahna JR (2008) *J Electrochem Soc* 155:A812
11. Manickam M, Takata M (2003) *Electrochim Acta* 48:957
12. Lestriez B, Bahri S, Sandu I, Roué L, Guyomard D (2007) *Electrochim Commun* 9:2801
13. Guerfi A, Kaneko M, Petitclerc M, Mori M, Zaghib K (2007) *J Power Sources* 163:1047
14. Chen L, Xie X, Xie J, Wang K, Yang J (2006) *J Appl Electrochem* 36:1099
15. Yuan L, Guo ZP, Konstantinov K, Munroe P, Liu HK (2006) *Electrochim Solid-State Lett* 9:A524
16. Ng SH, Wang J, Wexler D, Konstantinov K, Guo ZP, Liu HK (2006) *Angew Chem Int Ed* 45:6896
17. Huang XH, Tu JP, Zhang CQ, Xiang JY (2007) *Electrochim Commun* 9:1180